10.24425/acs.2022.142847

Archives of Control Sciences
Volume 32(LXVIII), 2022
No. 3, *pages* 507–534

A new 4-D hyperchaotic four-wing system, its bifurcation analysis, complete synchronization and circuit simulation

Sundarapandian VAIDYANATHAN, Khaled BENKOUIDER,
Aceng SAMBAS and Samy Abdelwahab SAFAAN

In this work, we modify the dynamics of 3-D four-wing Li chaotic system (Li *et al.* 2015) by introducing a feedback controller and obtain a new 4-D hyperchaotic four-wing system with complex properties. We show that the new hyperchaotic four-wing system have three saddle-foci balance points, which are unstable. We carry out a detailed bifurcation analysis for the new hyperchaotic four-wing system and show that the hyperchaotic four-wing system has multistability and coexisting attractors. Using integral sliding mode control, we derive new results for the master-slave synchronization of hyperchaotic four-wing systems. Finally, we design an electronic circuit using MultiSim for real implementation of the new hyperchaotic four-wing system.

Key words: multistability, Hyperchaos, four-wing systems, hyperchaotic systems, synchronization, sliding mode control and circuit design

1. Introduction

Hyperchaotic systems have a wide range of engineering applications due to their high complexity [1]. Djimasra *et al.* [2] reported a digital image cryptosystem using a hyperchaotic Lorenz oscillator and discussed the various security

S. Vaidyanathan (corresponding author, e-mail: sundarvtu@gmail.com) is with School of Electrical and Computing, Vel Tech University, 400 Feet Outer Ring Road, Avadi, Chennai-600092, Tamil Nadu, India.

K. Benkouider (e-mail: benkouider.khaled@gmail.com) is with Non Destructive Testing Laboratory, Automatic Department, Jijel University, BP 98, 18000, Jijel, Algeria.

A. Sambas (e-mail: acengs@umtas.ac.id) is with Department of Mechanical Engineering, Universitas Muhammadiyah Tasikmalaya, Tasikmalaya 46196, West Java, Indonesia.

S.A. Safaan (e-mail: safan@qu.edu.sa) is with Department of Natural and Applied Sciences, Community College of Buraydah, Qassim University, Buraydah, 52571, Saudi Arabia and Nile Higher Institute for Commercial Science and Computer Technology, Mansoura, 35511, Egypt.

Received 06.11.2021. Revised 09.08.2022.

issues with their robust cryptosystem. Petrzela [3] discussed on a new hyperchaotic oscillator which is based on the topology of a two-stage amplifier. McCullen and Moresco [4] studied hyperchaos in a system of coupled electronic chaotic oscillators with multistability. Abdulkadhim and Shehab [5] proposed a steganographic method based on a 4-D multi-wing hyperchaotic system. Gupta and Chauhan [6] proposed a secure image encryption algorithm based on 4-D hyperchaotic systems. Bian and Yu [7] suggested a 6-D hyperchaotic system based on a 4-D hyperchaotic Lorenz system and designed a new communication encryption method with the 6-D hyperchaotic system. Zhang *et al.* [8] designed a lossless image encryption and compression scheme using a hyperchaotic system. Khan and Kumar [9] discussed a study of chaos in a satellite system, which has important applications.

Li *at al.* (2015) proposed a new 3-D four-wing chaotic system with three quadratic nonlinear terms. In this work, we propose a new 4-D hyperchaotic four-wing system by adding a feedback control to the Li chaotic system [10]. Bifurcation analysis helps to understand the novel features of new chaotic and hyperchaotic systems [11–13]. We carry out a detailed bifurcation analysis of the new 4-D hyperchaotic four-wing system and describe the changes in the qualitative properties of the new hyperchaotic four-wing system by varying the parameter values. Recently, there is significant interest in reporting chaotic and hyperchaotic systems having multistability property [14–16]. In this work, we exhibit that the new hyperchaotic four-wing system has multistability with coexisting hyperchaotic attractors.

Synchronization of hyperchaotic systems has applications in areas such as cryptosystems [17, 18] and secure communication systems [19, 20]. In this work, we use integral sliding mode control for the master-slave synchronization of the new hyperchaotic four-wing systems. Sliding mode control is useful due to its attractive features such as robustness and insensitivity to small parameter variations, etc [21–28].

For real-world applications, we have designed an electronic circuit of the new hyperchaotic four-wing system using MultiSim. Circuit design of hyperchaotic systems is useful in practical applications [29, 30].

2. A new 4-D hyperchaotic four-wing system

In 2015, Li *et al.* [10] proposed a new 3-D four-wing system which is modelled by the dynamics

$$\begin{cases} \dot{y}_1 = a y_1 + y_2 + y_2 y_3 \,, \\ \dot{y}_2 = (y_2 - y_1) y_3 \,, \\ \dot{y}_3 = -y_3 - m y_1 y_2 + b. \end{cases} \tag{1}$$

It was shown in [10] that the Li system (1) exhibits a chaotic four-wing attractor when we take the parameter values as

$$a = 1, \qquad b = 1, \qquad m = 1. \tag{2}$$

For $(a, b, m) = (1, 1, 1)$ and $Y(0) = (0.4, 0.2, 0.4)$ and $T = 1E5$ sec, we found the Lyapunov exponents of the Li system (1) numerically as follows:

$$\mu_1 = 0.4093, \qquad \mu_2 = 0, \qquad \mu_3 = -1.7772. \tag{3}$$

Thus, the Li system (1) has a chaotic attractor with maximal Lyapunov exponent (MLE) as $\mu_1 = 0.4093$.

For MATLAB simulations, we take $(a, b, m) = (1, 1, 1)$ and $Y(0) = (0.4, 0.2, 0.4)$.

The phase portraits of the Li system (1) are shown in Figure 1.

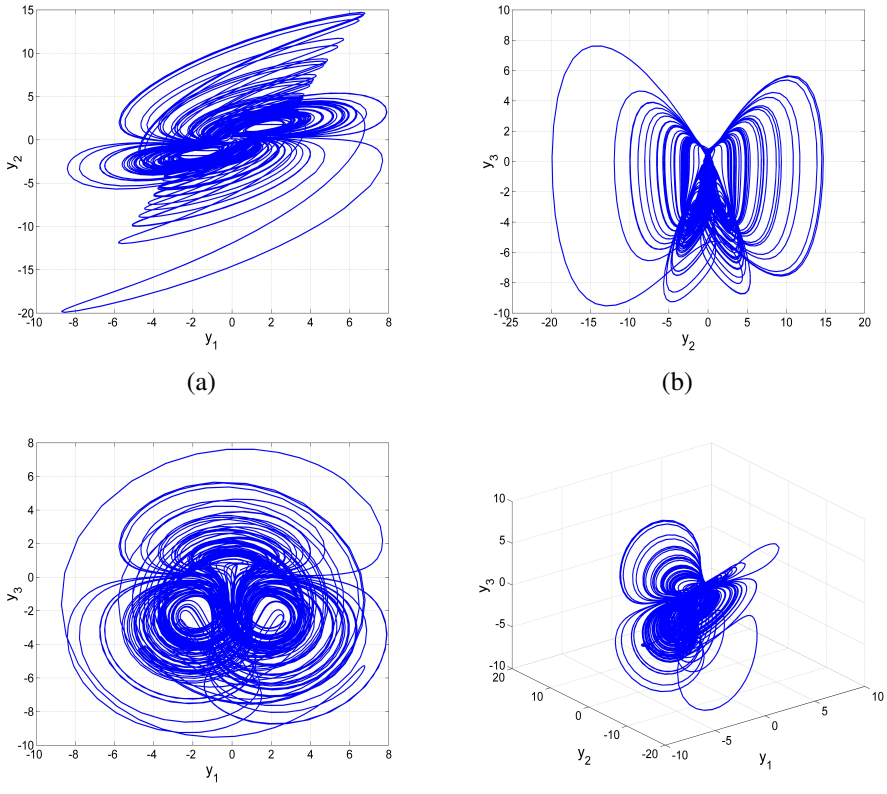

Figure 1: MATLAB signal plots of the four-wing Li chaotic system (1) for $Y(0) = (0.4, 0.2, 0.4$ and $(a, b, m) = (1, 1, 1)$: (a) (y_1, y_2)-plane, (b) (y_2, y_3)-plane, (c) (y_1, y_3)-plane, (d) the 3-D space

It is clear that the Li system (1) has a four-wing chaotic attractor.

In this work, we suggest a new 4-D system by introducing a new feedback controller y_4 to the Li system (1) and our system dynamics is described below:

$$\begin{cases} \dot{y}_1 = ay_1 + y_2 + y_2y_3 - y_4\,, \\ \dot{y}_2 = (y_2 - y_1)y_3\,, \\ \dot{y}_3 = -y_3 - my_1y_2 - py_2^2 + b, \\ \dot{y}_4 = y_1\,. \end{cases} \tag{4}$$

In the system (4), $Y = (y_1, y_2, y_3, y_4)$ is the state and a, b, c, m, p are positive parameters.

In this work, we shall establish that the system (4) has a hyperchaotic four-wing attractor for the constant values

$$a = 2.5, \quad b = 2.5, \quad c = 0.2, \quad m = 1, \quad p = 0.2. \tag{5}$$

For MATLAB simulations, we take the initial state as $Y(0) = (0.4, 0.2, 0.4, 0.2)$.

The Lyapunov exponents (LE) of the 4-D system (4) were calculated for $(a, b, c, m, p) = (2.5, 2.5, 0.2, 1, 0.2)$, $Y(0) = (0.4, 0.2, 0.4, 0.2)$ and $T = 1E5$ seconds as follows:

$$\mu_1 = 0.5292, \qquad \mu_2 = 0.0735, \qquad \mu_3 = 0, \qquad \mu_4 = -3.4444. \tag{6}$$

From (6), we deduce that the 4-D system (4) has two positive LE values, μ_1 and μ_2.

Moreover $\mu_1 + \mu_2 + \mu_3 + \mu_4 < 0$.

Thus, the 4-D system (4) has a dissipative hyperchaotic attractor with maximal Lyapunov exponent (MLE) as $\mu_1 = 0.5292$. We observe that the MLE of the 4-D hyperchaotic system given by $\mu_1 = 0.5292$ is greater than the MLE of the 3-D Li chaotic system given by $\mu_1 = 0.4093$.

For the signal plots in MATLAB, we take

$$(a, b, c, m, p) = (2.5, 2.5, 0.2, 1, 0.2) \quad \text{and} \quad Y(0) = (0.4, 0.2, 0.4, 0.2).$$

The phase portraits of the new hyperchaotic system (4) are shown in Figure 2.

It is clear that the new hyperchaotic system (4) has a four-wing hyperchaotic attractor.

We remark that the new hyperchaotic four-wing system (4) is invariant under the change of coordinates

$$(y_1, y_2, y_3, y_4) \mapsto (-y_1, -y_2, y_3, -y_4). \tag{7}$$

This shows that the hyperchaotic four-wing system (4) has rotation symmetry about the y_3-coordinate axis.

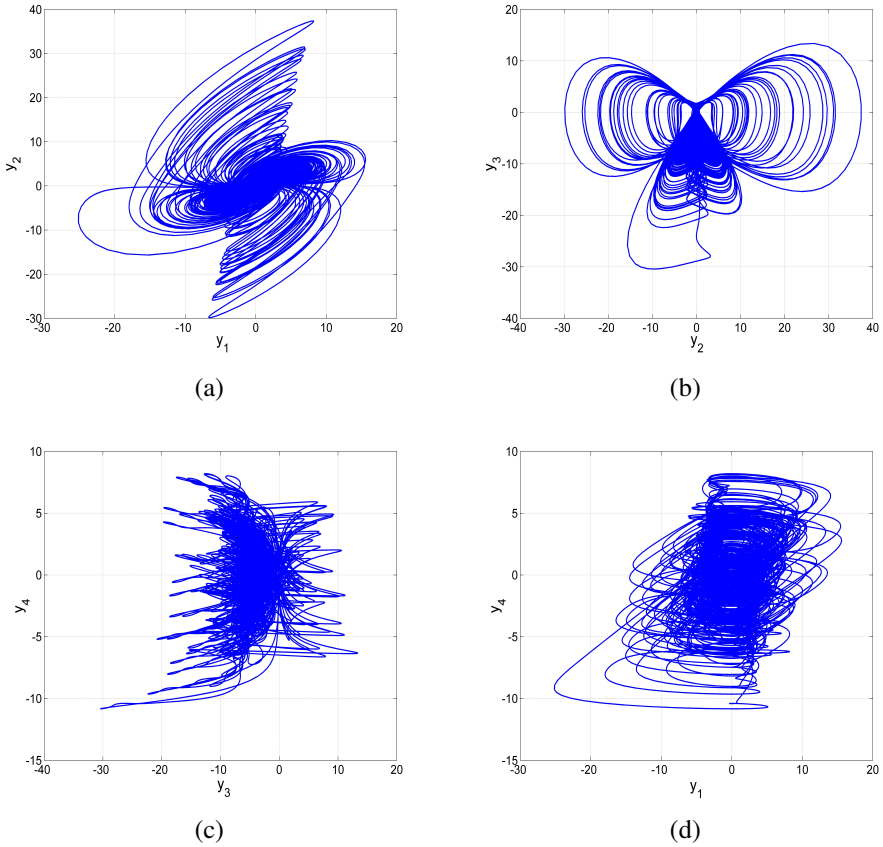

Figure 2: MATLAB signal plots of the hyperchaotic four-wing system (4) for $Y(0) = (0.4, 0.2, 0.4, 0.2)$ and $(a, b, c, m, p) = (2.5, 2.5, 0.2, 1, 0.2)$: (a) (y_1, y_2)-plane, (b) (y_2, y_3)-plane, (c) (y_3, y_4)-plane, (d) (y_1, y_4)-plane

To find the balance points of the hyperchaotic four-wing system (4), we solve the equations $\dot{y}_1 = 0$, $\dot{y}_2 = 0$, $\dot{y}_3 = 0$ and $\dot{y}_4 = 0$ when the system parameters are positive.

Thus, we solve the following system of equations:

$$ay_1 + y_2 + y_2y_3 - y_4 = 0, \tag{8a}$$

$$-cy_1 + (y_2 - y_1)y_3 = 0, \tag{8b}$$

$$-y_3 - my_1y_2 - py_2^2 + b = 0, \tag{8c}$$

$$y_1 = 0. \tag{8d}$$

From (8d), it is clear that $y_1 = 0$.

Hence, the balance points of the 4-D system (4) lie on the (y_2, y_3, y_4)-space.

Substituting $y_1 = 0$ into (8b), we get $y_2 y_3 = 0$. Either $y_2 = 0$ or $y_3 = 0$.

Thus, we have two cases to consider.

Case A: $y_2 = 0$.

Putting $y_1 = 0$ and $y_2 = 0$ in Eq. (8a), we get $y_4 = 0$.

Putting $y_1 = 0$ and $y_2 = 0$ in Eq. (8c), we get $y_3 = b$.

Thus, $E_1 = (0, 0, b, 0)$ is a balance point of the system (4).

Case B: $y_3 = 0$.

Putting $y_1 = 0$ and $y_3 = 0$ in Eq. (8a), we get $y_2 = y_4$.

Putting $y_1 = 0$ and $y_3 = 0$ in Eq. (8c), we get $py_2^2 = b$.

Solving, we get $y_2 = \pm\sqrt{\frac{b}{p}}$.

Thus, $E_2 = \left(0, \sqrt{\frac{b}{p}}, 0, \sqrt{\frac{b}{p}}\right)$ and $E_3 = \left(0, -\sqrt{\frac{b}{p}}, 0, -\sqrt{\frac{b}{p}}\right)$ are two more balance points of the hyperchaotic system (4).

Combining Cases A and B, we conclude that E_1, E_2 and E_3 are three balance points of the hyperchaotic system (4).

For the hyperchaotic case, we take the parameters as in (5).

In this case, the three balance points take the numerical form:

$$E_1 = \begin{bmatrix} 0 \\ 0 \\ 2.5 \\ 0 \end{bmatrix}, \qquad E_2 = \begin{bmatrix} 0 \\ 3.5355 \\ 0 \\ 3.5355 \end{bmatrix}, \qquad E_3 = \begin{bmatrix} 0 \\ -3.5355 \\ 0 \\ -3.5355 \end{bmatrix}. \tag{9}$$

It is easy to verify that E_1, E_2 and E_3 are all saddle-foci balance points, which are unstable.

3. Lyapunov exponents and bifurcation analysis

In this section, the influence of the parameters on the behavior of the new 4-D hyperchaotic four-wing system (4) will be investigated using Lyapunov spectrums, bifurcation diagrams and phase plots.

3.1. Bifurcation analysis when a varies

Bifurcation diagram and Lyapunov epxonents spectrum of the hyperchaotic four-wing system (4) are plotted in Figure 3 when a varies in the region $[0, 3]$ while the other parameters are fixed as $b = 2.5$, $c = 0.2$, $m = 1$ and $p = 0.2$. We can see that the results obtained from the Lyapunov spectrum agree with the results given by the bifurcation diagram.

From Figure 3, we can see that system (4) is hyperchaotic for large region of parameter a values. In addition, the system (4) can evolve into periodic orbits and

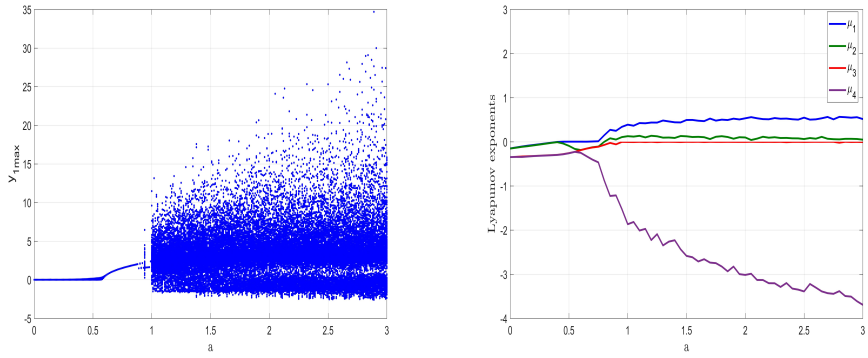

(a) (b)

Figure 3: Dynamic analysis of the hyperchaotic four-wing system (4) when $b = 2.5$, $c = 0.2$, $m = 1$, $p = 0.2$ and a varies in $[0, 3]$: (a) bifurcation diagram and (b) Lyapunov exponents spectrum

chaotic orbits or converge to its equilibrium. We can identify the behavior of the four-wing system (4) when parameter a varies as follows:

When $a \in [0, 0.4]$, the states of the system (4) converges to the equilibrium point E_2 and their corresponding Lyapunov exponents when $a = 0.1$ are:

$$\mu_1 = -0.106, \qquad \mu_2 = -0.113, \qquad \mu_3 = -0.332, \qquad \mu_4 = -0.344. \tag{10}$$

When $a \in [0.4, 0.75]$, there is one zero Lyapunov exponent and three negative Lyapunov exponents. This implies that system (4) generates periodic behavior with the following values of Lyapunov exponents obtained when $a = 0.5$:

$$\mu_1 = 0, \qquad \mu_2 = -0.092, \qquad \mu_3 = -0.255, \qquad \mu_4 = -0.259. \tag{11}$$

When $a \in [0.75, 0.85]$, the maximal Lyapunov exponent is positive, the second Lyapunov exponent is zero while the last two Lyapunov exponents are negative. This implies that the system (4) exhibits chaotic behavior with the following values of Lyapunov exponents obtained when $a = 0.8$:

$$\mu_1 = 0.148, \qquad \mu_2 = 0, \qquad \mu_3 = -0.069, \qquad \mu_4 = -0.875 \tag{12}$$

Finally, when $a \in [0.85, 3]$, we can confirm using results from Figure 3 that the system (4) has two positive Lyapunov exponents. This implies the existence of hyperchaos for the system (4). The values of Lyapunov exponents when $a = 2$ are:

$$\mu_1 = 0.533, \qquad \mu_2 = 0.099, \qquad \mu_3 = 0, \qquad \mu_4 = -3.015. \tag{13}$$

Figure 4 shows different signal plots corresponding to different behavior of the new hyperchaotic four-wing system (4) when a varies. Table 1 gives the

dynamics, Lyapunov exponents and Lyapunov dimension of the system (4) for different values of a.

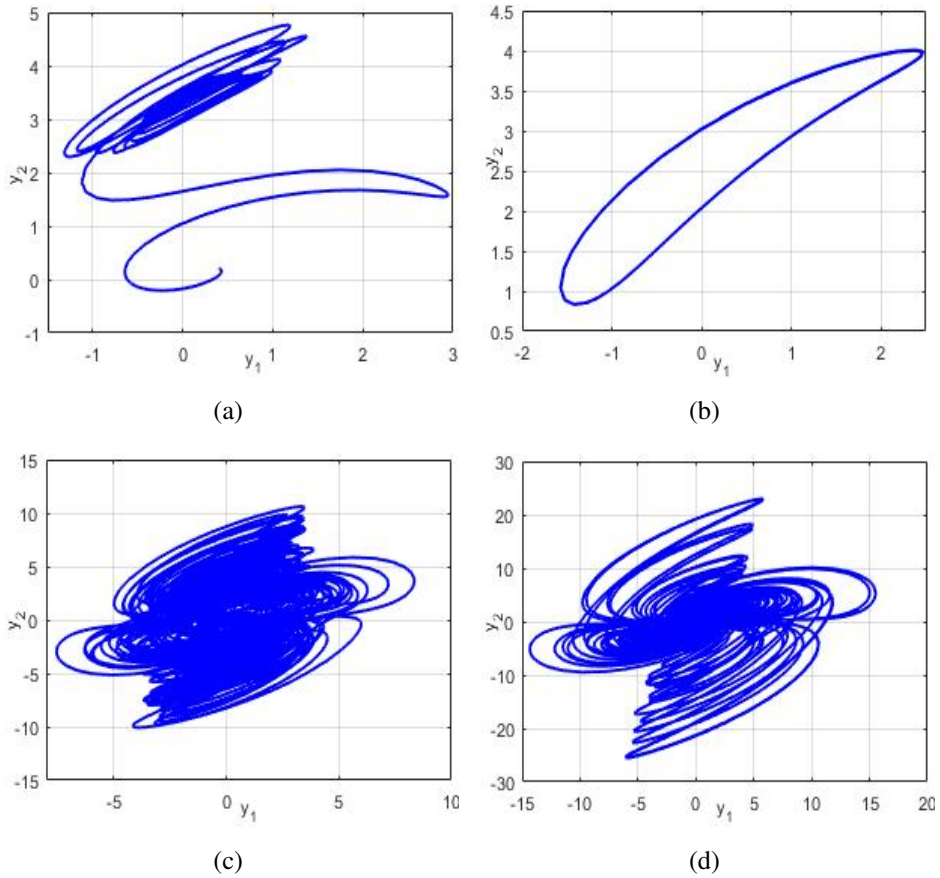

Figure 4: (y_1, y_2) – signal plots of the hyperchaotic four-wing system (4) when $b = 2.5$, $c = 0.2$, $m = 1$, $p = 0.2$: (a) E_2 attractor when $a = 0.1$, (b) periodic orbit when $a = 0.5$, (c) chaotic attractor when $a = 0.8$, (d) hyperchaotic attractor when $a = 2$

3.2. Bifurcation analysis when b varies

Bifurcation diagram and Lyapunov epxonents spectrum of the hyperchaotic four-wing system (4) are plotted in Figure 5 when b varies in the region $[-3, 3]$ while the other parameters are fixed as $a = 2.5$, $c = 0.2$, $m = 1$ and $p = 0.2$. We can see that the results obtained from the Lyapunov spectrum agree with the results given by the bifurcation diagram.

From Figure 5, we can see that system (4) is hyperchaotic for large region of parameter b values. In addition, the system (4) can evolve into periodic orbits,

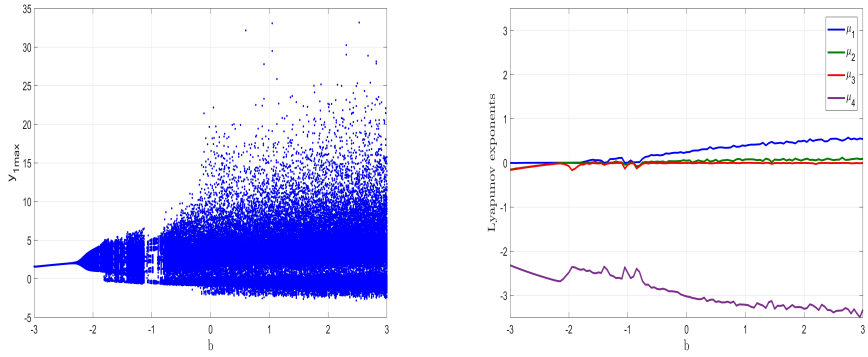

(a) (b)

Figure 5: Dynamic analysis of the hyperchaotic four-wing system (4) when $a = 2.5$, $c = 0.2$, $m = 1$, $p = 0.2$ and b varies in $[-3, 3]$: (a) bifurcation diagram and (b) Lyapunov exponents spectrum

quasi-periodic orbits or chaotic orbits. We can identify the behavior of the four-wing system (4) when parameter b varies as follows:

Define $A = [-3, -2.3] \cup [-1.4, -1.35] \cup [-1.05, -1] \cup [-0.9 \cup -0.8]$.

When $b \in A$, the states of the system (4) converges to a periodic orbit and their corresponding Lyapunov exponents when $b = -3$ are:

$$\mu_1 = 0, \qquad \mu_2 = -0.153, \qquad \mu_3 = -0.161, \qquad \mu_4 = -2.320. \tag{14}$$

When $b \in [-2.3, -1.8]$, there are two zero Lyapunov exponents and two negative Lyapunov exponents. This implies that system (4) evolves into quasi-periodic behavior with the following values of Lyapunov exponents obtained when $b = -1.8$:

$$\mu_1 = 0, \qquad \mu_2 = 0, \qquad \mu_3 = -0.038, \qquad \mu_4 = -2.423. \tag{15}$$

Define $B = [-1.8, -1.65] \cup [-1.35, -1.25] \cup [-1, -0.9]$.

When $b \in B$, the maximal Lyapunov exponent is positive, the second Lyapunov exponent is zero while the last two Lyapunov exponents are negative. This implies that the system (4) exhibits chaotic behavior with the following values of Lyapunov exponents obtained when $b = -1.68$.

$$\mu_1 = 0.058, \qquad \mu_2 = 0, \qquad \mu_3 = -0.010, \qquad \mu_4 = -2.442. \tag{16}$$

Define $C = [-1.65, -1.4] \cup [-1.25, -1.05] \cup [-0.8, 3]$.

Finally, when $b \in C$, we can confirm using results from Figure 5 that the system (4) has two positive Lyapunov exponents. This implies the existence of

hyperchaos for the system (4). The values of Lyapunov exponents when $b = 3$ are:

$$\mu_1 = 0.541, \qquad \mu_2 = 0.092, \qquad \mu_3 = 0, \qquad \mu_4 = -3.327. \tag{17}$$

Figure 6 shows different signal plots corresponding to different behavior of the new hyperchaotic four-wing system (4) when b varies. Table 1 gives the dynamics, Lyapunov exponents and Lyapunov dimension of the system (4) for different values of b.

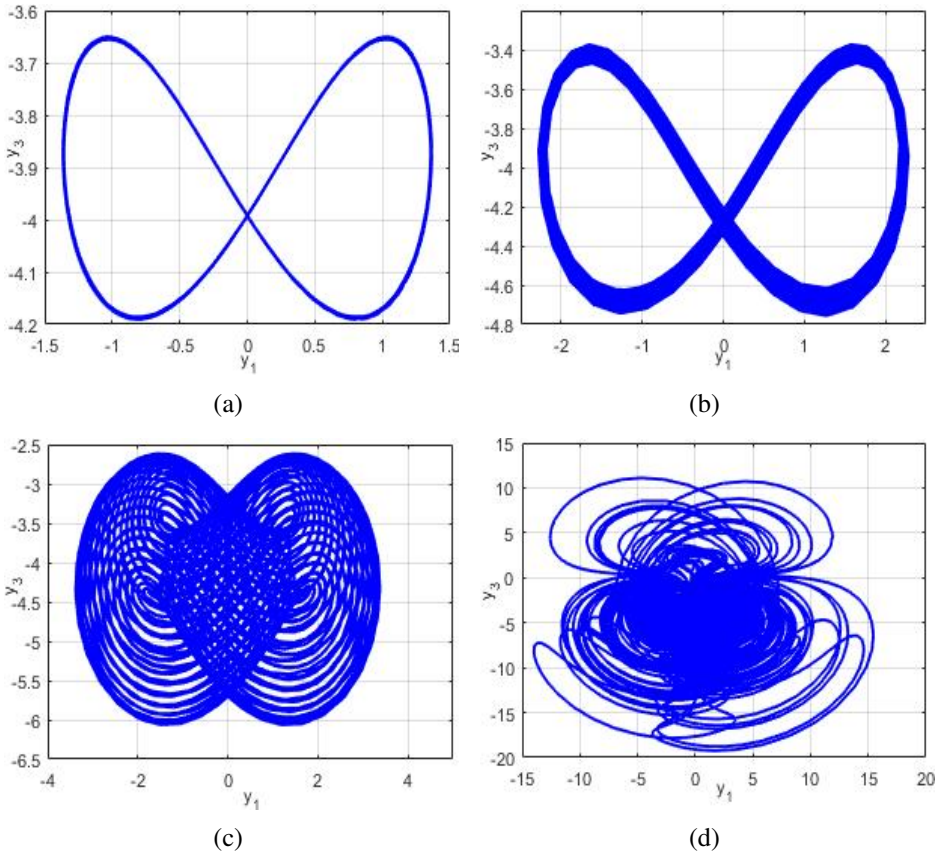

Figure 6: (y_1, y_3) – signal plots of the hyperchaotic four-wing system (4) when $a = 2.5$, $c = 0.2$, $m = 1$, $p = 0.2$: (a) periodic orbit when $b = -3$, (b) quasi-periodic orbit when $b = -1.8$, (c) Chaotic attractor when $b = -1.68$, (d) hyperchaotic attractor when $b = 3$

3.3. Bifurcation analysis when c varies

Bifurcation diagram and Lyapunov epxonents spectrum of the hyperchaotic four-wing system (4) are plotted in Figure 7 when c varies in the region $[0, 1.3]$ while the other parameters are fixed as $a = 2.5$, $b = 2.5$, $m = 1$ and $p = 0.2$.

We can see that the results obtained from the Lyapunov spectrum agree with the results given by the bifurcation diagram.

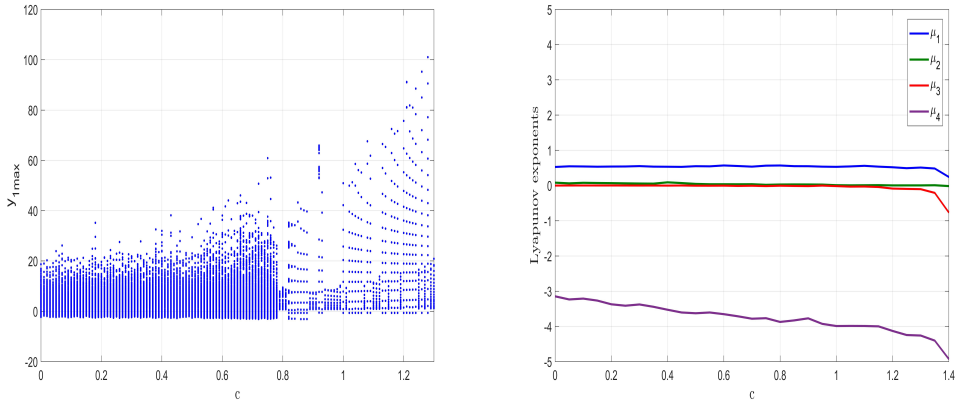

(a) (b)

Figure 7: Dynamic analysis of the hyperchaotic four-wing system (4) when $a = 2.5$, $b = 2.5, m = 1, p = 0.2$ and c varies in $[0, 1.3]$: (a) bifurcation diagram and (b) Lyapunov exponents spectrum

From Figure 7, we can see that system (4) is hyperchaotic for almost all the region of parameter values of c in $[0, 1.3]$. In addition, the system (4) can exhibit periodic behavior for the rest of the parameter c region in $[0, 1.3]$. We can identify the behavior of the four-wing system (4) when parameter c varies as follows:

When $c \in [0, 1]$, the system (4) has two positive Lyapunov exponents, one zero Lyapunov exponent and one negative Lyapunov exponent. This implies the existence of hyperchaos for the system (4). The values of Lyapunov exponents when $c = 0.4$ are:

$$\mu_1 = 0.516, \qquad \mu_2 = 0.098, \qquad \mu_3 = 0, \qquad \mu_4 = -3.511. \tag{18}$$

When $c \in [1, 1.3]$, we can see from Figure 7 that the four-wing system (4) has only one positive Lyapunov exponent. Thus, the system (4) evolves into a chaotic attractor and the values of Lyapunov exponents obtained when $c = 1.3$ are:

$$\mu_1 = 0.478, \qquad \mu_2 = 0, \qquad \mu_3 = -0.097, \qquad \mu_4 = -4.313. \tag{19}$$

Figure 8 shows different phases plots corresponding to different behavior of the new hyperchaotic four-wing system (4) when c varies. Table 1 gives the dynamics, Lyapunov exponents and Lyapunov dimension of the system (4) for different values of c.

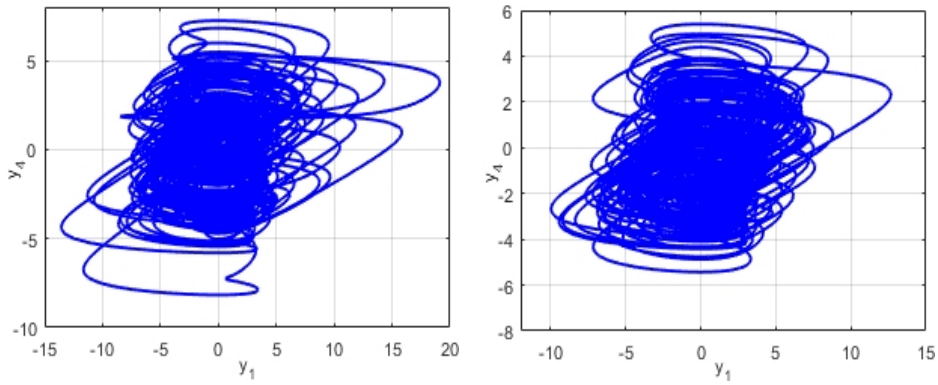

(a) (b)

Figure 8: (y_1, y_4) – signal plots of the hyperchaotic four-wing system (4) when $a = 2.5$, $b = 2.5$, $m = 1$ and $p = 0.2$. (a) Hyperchaotic attractor for $c = 0.4$ and (b) chaotic attractor for $c = 1.3$

3.4. Bifurcation analysis when m varies

Bifurcation diagram and Lyapunov epxonents spectrum of the hyperchaotic four-wing system (4) are plotted in Figure 9 when m varies in the region $[0.4, 1]$ while the other parameters are fixed as $a = 2.5$, $b = 2.5$, $c = 0.2$ and $p = 0.2$. We can see that the results obtained from the Lyapunov spectrum agree with the results given by the bifurcation diagram.

From Figure 9, we can see that system (4) can generate chaotic or hyperchaotic attractor when m varies. We can identify the behavior of the system (4) when the parameter m varies as follows:

When $m \in [0.4, 0.5]$, the maxinal Lyapunov exponent is positive, the second Lyapunov exponent is zero, while the last two Lyapunov exponents are negative. This means that the system (4) evolves into a chaotic attractor with the following values of Lyapunov exponents obtained when $m = 0.45$:

$$\mu_1 = 0.248, \qquad \mu_2 = 0, \qquad \mu_3 = -0.282, \qquad \mu_4 = -3.612. \tag{20}$$

When $m \in [0.5, 1]$, we can see from Figure 9 that the four-wing system (4) has two positive Lyapunov exponents. Thus, the system (4) evolves into a hyperchaotic attractor and the values of Lyapunov exponents obtained when $m = 0.75$ are:

$$\mu_1 = 0.502, \qquad \mu_2 = 0.079, \qquad \mu_3 = 0, \qquad \mu_4 = -3.420. \tag{21}$$

Figure 10 shows different phases plots corresponding to different behavior of the new hyperchaotic four-wing system (4) when c varies. Table 1 gives the dynamics, Lyapunov exponents and Lyapunov dimension of the system (4) for different values of m.

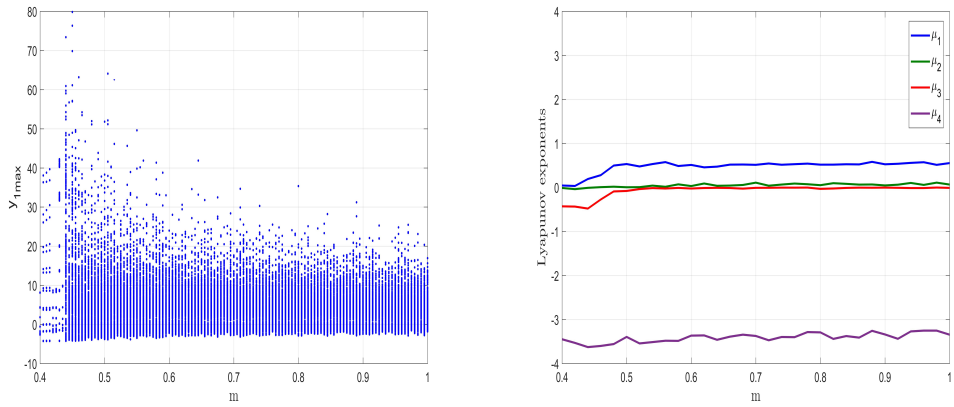

(a) (b)

Figure 9: Dynamic analysis of the hyperchaotic four-wing system (4) when $a = 2.5$, $b = 2.5$, $c = 0.2$, $p = 0.2$ and m varies in $[0.4, 1]$: (a) bifurcation diagram and (b) Lyapunov exponents spectrum

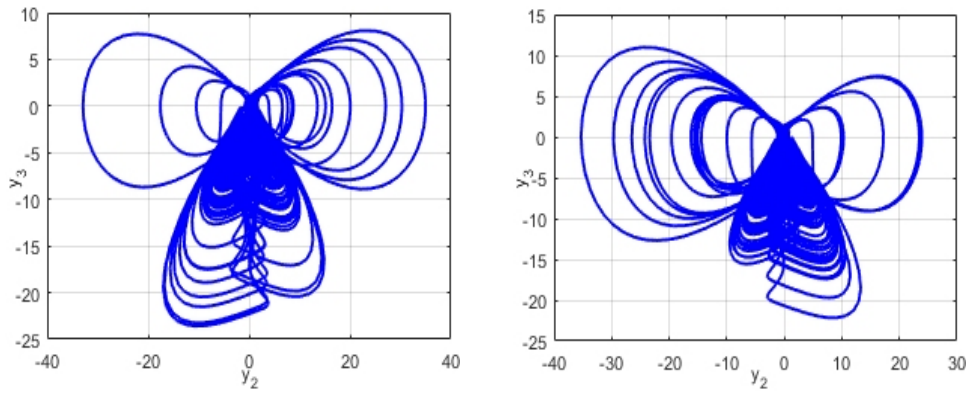

(a) (b)

Figure 10: (y_2, y_3) – signal plots of the hyperchaotic four-wing system (4) when $a = 2.5$, $b = 2.5$, $c = 0.2$ and $p = 0.2$. (a) Chaotic attractor for $m = 0.45$ and (b) Hyperchaotic attractor for $m = 0.75$

3.5. Bifurcation analysis when p varies

Bifurcation diagram and Lyapunov epxonents spectrum of the hyperchaotic four-wing system (4) are plotted in Figure 11 when p varies in the region $[0, 0.4]$ while the other parameters are fixed as $a = 2.5$, $b = 2.5$, $c = 0.2$ and $m = 1$. We can see that the results obtained from the Lyapunov spectrum agree with the results given by the bifurcation diagram.

From Figure 11, we can see that system (4) can generate hyperchaotic or chaotic attractor when p varies. We can identify the behavior of the system (4) when the parameter p varies as follows:

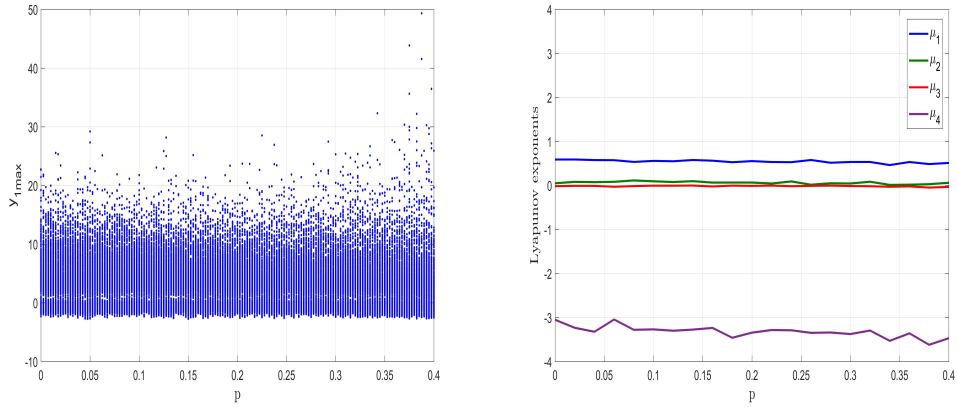

(a) (b)

Figure 11: Dynamic analysis of the hyperchaotic four-wing system (4) when $a = 2.5$, $b = 2.5$, $c = 0.2$, $m = 1$ and p varies in $[0, 0.4]$: (a) bifurcation diagram and (b) Lyapunov exponents spectrum

When $p \in [0, 0.34]$, we can see from Figure 11 that the four-wing system (4) has two positive Lyapunov exponents. Thus, the system (4) evolves into a hyperchaotic attractor and the values of Lyapunov exponents obtained when $p = 0.2$ are:

$$\mu_1 = 0.548, \qquad \mu_2 = 0.063, \qquad \mu_3 = 0, \qquad \mu_4 = -3.389 \tag{22}$$

When $p \in [0.34, 4]$, the maxinal Lyapunov exponent is positive, the second Lyapunov exponent is zero, while the last two Lyapunov exponents are negative. This means that the system (4) evolves into a chaotic attractor with the following values of Lyapunov exponents obtained when $p = 0.37$ are:

$$\mu_1 = 0.509, \qquad \mu_2 = 0, \qquad \mu_3 = -0.051, \qquad \mu_4 = -3.558 \tag{23}$$

Figure 12 shows different phases plots corresponding to different behavior of the new hyperchaotic four-wing system (4) when c varies. Table 1 gives the dynamics, Lyapunov exponents and Lyapunov dimension of the system (4) for different values of p.

Table 1: Dynamics and Lyapunov Exponents of the 4-D System (4) versus its Parameters

Dynamics	Parameters					Bifurcation parameter	Lyapunov Exponents				L_D	Attractor
	a	b	c	m	p		μ_1	μ_2	μ_3	μ_4		
Periodic	[0.4, 0.75]	2.5	0.2	1	0.2	$a = 0.1$	0	−0.092	−0.255	−0.259	0	Fig. 4(b)
	2.5	A	0.2	1	0.2	$b = 3$	0	−0.153	−0.161	−2.320	0	Fig. 6(a)
Quasi-periodic	2.5	[−2.3, −1.8]	0.2	1	0.2	$b = -1.8$	0	0	−0.038	−2.423	0	Fig. 6(b)
Chaos	[0.75, 0.85]	2.5	0.2	1	0.2	$a = 0.8$	0.148	0	−0.069	−0.875	3.090	Fig. 4(c)
	2.5	B	0.2	1	0.2	$b = 1.68$	0.058	0	−0.010	−2.442	3.019	Fig. 6(c)
	2.5	2.5	[1, 1.3]	1	0.2	$c = 1.3$	0.478	0	−0.097	−4.313	3.088	Fig. 8(b)
	2.5	2.5	0.2	[0.4, 0.5]	0.2	$m = 0.46$	0.248	0	−0.282	−3.612	2.879	Fig. 10(a)
	2.5	2.5	0.2	1	[0.34, 0.4]	$p = 0.37$	0.509	0	−0.051	−3.558	3.058	Fig. 12(b)
Hyperchaos	[0.85, 3]	2.5	0.2	1	0.2	$a = 2$	0.533	0.099	0	−3.015	3.209	Fig. 4(d)
	2.5	C	0.2	1	0.2	$b = 3$	0.541	0.092	0	−3.327	3.190	Fig. 6(d)
	2.5	2.5	[0, 1]	1	0.2	$c = 0.4$	0.516	0.098	0	−3.511	3.176	Fig. 8(a)
	2.5	2.5	0.2	[0.5, 1]	0.2	$m = 0.75$	0.502	0.079	0	−3.420	3.170	Fig. 10(b)
	2.5	2.5	0.2	1	[0, 0.34]	$p = 0.2$	0.548	0.063	0	−3.389	3.276	Fig. 12(a)

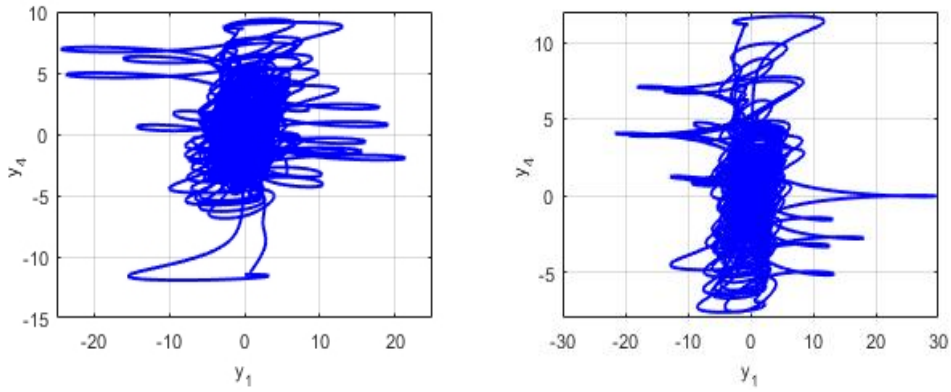

(a) (b)

Figure 12: (y_1, y_4) – signal plots of the hyperchaotic four-wing system (4) when $a = 2.5$, $b = 2.5$, $c = 0.2$ and $m = 1$: (a) hyperchaotic attractor for $p = 0.2$ and (b) chaotic attractor for $p = 0.37$

4. Multistability phenomenon in the hyperchaotic four-wing system

In order to observe the strange phenomenon of multistability, the attractors of the new four-wing system (4) are calculated for two different initial values and plotted using Matlab software.

As we mentioned in Section 2, the new system (4) is invariant under the transformation

$$F\colon (y_1, y_2, y_3, y_4) \mapsto (-y_1, -y_2, y_3, -y_4). \tag{24}$$

Thus, a good choice of two different initial conditions can give rise to the appearance of coexisting attractors. Let X_0 and Y_0 be two different initial conditions for the new four-wing system (4), where $X_0 = (1, 1, 1, 1)$ generates a blue color orbit and $Y_0 = (-1, -1, 1, -1)$ generates a red color orbit.

When we set $b = 2.5$, $c = 0.2$, $m = 1$, $p = 0.2$and vary a in the range $[0, 3]$, the system (4) exhibits coexistence of point attractors, periodic attractors, chaotic attractors or hyperchaotic attractors starting from the two different initial points X_0 (blue color) and Y_0 (red color).

When $a = 0.1$, the system (4) exhibits two coexisting point attractors, where the blue one converges to the balance point E_2 while the red one converges to E_3 as clearly shown in Figure 13(a).

When $a = 0.5$, the system (4) generates two coexisting periodic attractors, the blue one starts from X_0 while the other one starts from Y_0. Results are depicted in Figure 13(b).

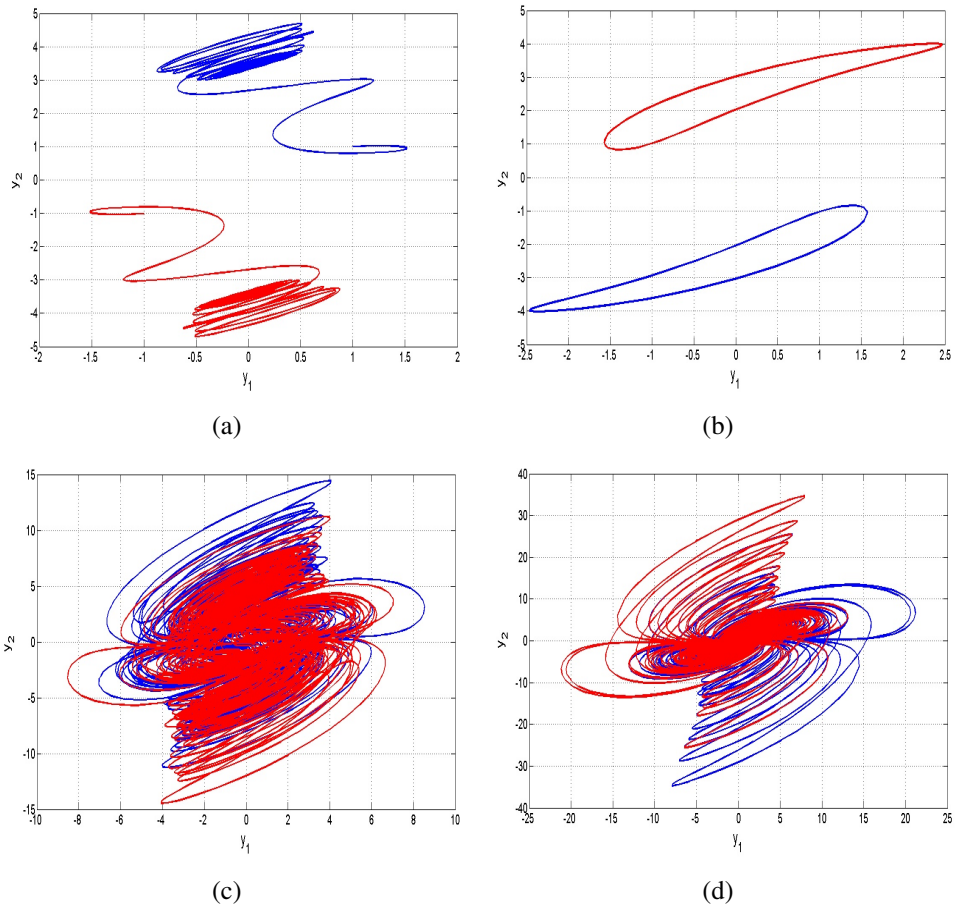

Figure 13: MATLAB phase plots of various coexisting attractors of the system (4) in the (y_1, y_2) plane: (a) point attractors for $a = 0.1$, (b) periodic attractors for $a = 0.5$, (c) chaotic attractors for $a = 0.78$ and (d) hyperchaotic attractors for $a = 2.5$

When $a = 0.78$, the four-wing system (4) generates two coexisting chaotic attractors as Figure 13(c) shows. Each attractor has only one positive Lyapunov exponents as follows:

$$\mu_1 = 0.148, \qquad \mu_2 = 0, \qquad \mu_3 = -0.069, \qquad \mu_4 = -0.875. \tag{25}$$

Finally, when $a = 2.5$, the proposed system (4) generates two coexisting hyperchaotic attractors as shown in Figure 13(d). The blue attractor starts from X_0 while the red attractor starts from Y_0. These two coexisting attractors are characterised by the following values of Lyapunov exponents:

$$\mu_1 = 0.547, \qquad \mu_2 = 0.060, \qquad \mu_3 = 0, \qquad \mu_4 = -3.404. \tag{26}$$

5. Offset Boosting Property of the New Hyperchaotic Four-Wing System

Clearly, we can boost the variable y_4 of the new hyperchaotic four-wing system (4) as it appears only once in the first equation of the system. Therefore, we can control it using a control parameter g.

The offset-boosted system is obtained from the hyperchaotic four-wing system (4) by replacing y_4 with (y_4+g) in the first equation of the system (4). The offset-boosted system is given as follows:

$$\begin{cases} \dot{y}_1 = ay_1 + y_2 + y_2y_3 - (y_4 + g), \\ \dot{y}_2 = (y_2 - y_1)y_3\,, \\ \dot{y}_3 = -y_3 - my_1y_2 - py_2^2 + b, \\ \dot{y}_4 = y_1\,. \end{cases} \tag{27}$$

Here, g is a control parameter, which plays the role of offset-boosting controller.

For $a = 2.5$, $b = 2.5$, $c = 0.2$, $m = 1$, $p = 0.2$ and $Y_0 = (0.4, 0.2, 0.4, 0.2)$, the hyperchaotic signal y_4 can be boosted from a bipolar signal to a unipolar signal as shown in Figure 14 (a) by varying g in different directions. In addition, the locations of signal portraits of the hyperchaotic four-wing attractors can be adjusted by changing the value of the constant controller g. These results are plotted in the (y_3, y_4)-plane and shown in the Figure 14 (b).

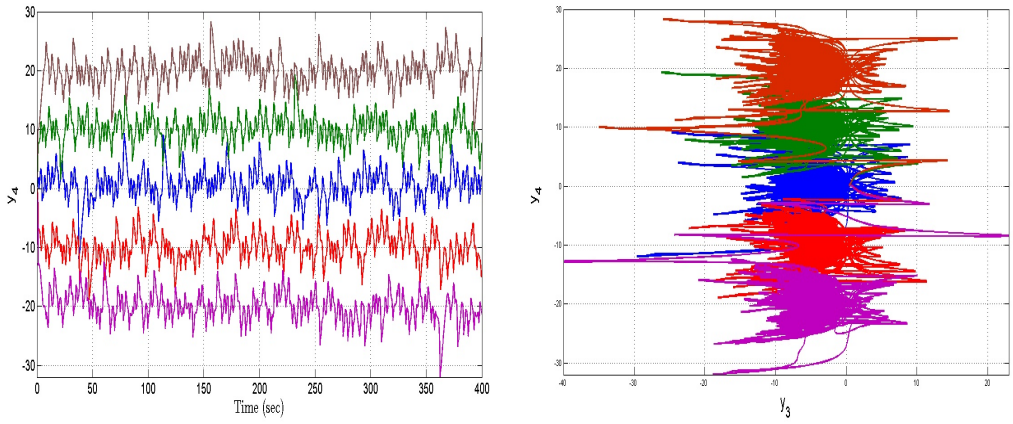

(a) (b)

Figure 14: Offset Boosting Plots: (a) y_4 signal and (b) (y_3, y_4) phase portraits of the system with different values of offset boosting controller: $g = 0$ (blue), $g = 10$ (red), $g = -10$ (green), $g = 20$ (violet) and $g = -20$ (brown)

6. Master-slave synchronisation of new hyperchaotic four-wing systems

Integral sliding mode control (ISMC) is successfully applied to achieve global synchronisation of the master hyperchaotic system (**M**) and slave hyperchaotic system (**S**) in this section.

$$(\mathbf{M})\begin{cases}\dot{y}_1 = ay_1 + y_2 + y_2y_3 - y_4\,,\\ \dot{y}_2 = (y_2 - y_1)y_3\,,\\ \dot{y}_3 = -y_3 - my_1y_2 - py_2^2 + b,\\ \dot{y}_4 = y_1\,;\end{cases} \tag{28}$$

$$(\mathbf{S})\begin{cases}\dot{z}_1 = az_1 + z_2 + z_2z_3 - z_4 + U_1\,,\\ \dot{z}_2 = (z_2 - z_1)z_3 + U_2\,,\\ \dot{z}_3 = -z_3 - mz_1z_2 - pz_2^2 + b + U_3\,,\\ \dot{z}_4 = z_1 + U_4\,.\end{cases} \tag{29}$$

Here, U_1, U_2, U_3, U_4 are integral sliding mode controls (ISMC) which will be designed so as to synchronize the states of the master system (M) and the slave system (S).

The synchronisation error between the systems (M) and (S) is defined as follows:

$$\begin{cases}E_1 = z_1 - y_1\,,\\ E_2 = z_2 - y_2\,,\\ E_3 = z_3 - y_3\,,\\ E_4 = z_4 - y_4\,.\end{cases} \tag{30}$$

The error dynamics is obtained as follows:

$$\begin{cases}\dot{E}_1 = aE_1 + E_2 - E_4 + z_2z_3 - y_2y_3 + U_1\,,\\ \dot{E}_2 = z_2z_3 - y_2y_3 - z_1z_3 + y_1y_3 + U_2\,,\\ \dot{E}_3 = -E_3 - m(z_1z_2 - y_1y_2) - p(z_2^2 - y_2^2) + U_3\,,\\ \dot{E}_4 = E_1 + U_4\,.\end{cases} \tag{31}$$

With each error variable, we link an integral sliding surface as follows:

$$\begin{cases} S_1 = E_1 + m_1 \int\limits_0^t E_1(\nu)\,\mathrm{d}\nu, \\ S_2 = E_2 + m_2 \int\limits_0^t E_2(\nu)\,\mathrm{d}\nu, \\ S_3 = Es_3 + m_3 \int\limits_0^t E_3(\nu)\,\mathrm{d}\nu, \\ S_4 = E_4 + m_4 \int\limits_0^t E_4(\nu)\,\mathrm{d}\nu. \end{cases} \tag{32}$$

By differentiation of the equations (32), we get

$$\begin{cases} \dot{S}_1 = \dot{E}_1 + \nu_1 E_1\,, \\ \dot{S}_2 = \dot{E}_2 + \nu_2 E_2\,, \\ \dot{S}_3 = \dot{E}_3 + \nu_3 E_3\,, \\ \dot{S}_4 = \dot{E}_4 + \nu_4 E_4\,. \end{cases} \tag{33}$$

The integral sliding mode controls for the master-slave synchronisation are defined as follows:

$$\begin{cases} U_1 = -aE_1 - E_2 + E_4 - z_2z_3 + y_2y_3 - \nu_1 E_1 - \alpha_1 \operatorname{sgn}(S_1) - \beta_1 S_1\,, \\ U_2 = -z_2z_3 + y_2y_3 + z_1z_3 - y_1y_3 - \nu_2 E_2 - \alpha_2 \operatorname{sgn}(S_2) - \beta_2 S_2\,, \\ U_3 = E_3 + m(z_1z_2 - y_1y_2) + p(z_2^2 - y_2^2) - \nu_3 E_3 - \alpha_3 \operatorname{sgn}(S_3) - \beta_3 S_3\,, \\ U_4 = -E_1 - \nu_4 E_4 - \alpha_4 \operatorname{sgn}(S_4) - \beta_4 S_4\,. \end{cases} \tag{34}$$

By implementing the sliding control law (34), we derive the following closed-loop system:

$$\begin{cases} \dot{E}_1 = -\nu_1\,\epsilon_1 - \alpha_1 \operatorname{sgn}(S_1) - \beta_1 S_1\,, \\ \dot{E}_2 = -\nu_2\,\epsilon_2 - \alpha_2 \operatorname{sgn}(S_2) - \beta_2 S_2\,, \\ \dot{E}_3 = -\nu_3\,\epsilon_3 - \alpha_3 \operatorname{sgn}(S_3) - \beta_3 S_3\,, \\ \dot{E}_4 = -\nu_4\,\epsilon_4 - \alpha_4 \operatorname{sgn}(S_4) - \beta_4 S_4\,. \end{cases} \tag{35}$$

Theorem 1 *The master-slave 4-D hyperchaotic models (28) and (28) are asymptotically and globally synchronised by the integral sliding mode control law (34) where ν_i, p_i, q_i, $(i = 1, 2, 3, 4)$ are assumed to be positive constants.*

Proof. We regard the Lyapunov function given by the definition

$$V(S_1, S_2, S_3, S_4) = \frac{1}{2}\left(S_1^2 + S_2^2 + S_3^2 + S_4^2\right) \tag{36}$$

which is evidently a strictly positive definite function on $\mathbb{R}^4$.

We observe next that

$$\dot{V} = S_1\dot{S}_1 + S_2\dot{S}_2 + S_3\dot{S}_3 + S_4\dot{S}_4\,. \tag{37}$$

Using (33) and (35), we can simplify (37) as

$$\dot{V} = \sum_{i=1}^{4} S_i\left(-\alpha_i \operatorname{sgn}(S_i) - \beta_i S_i\right). \tag{38}$$

A simplification shows that

$$\dot{V} = -\sum_{i=1}^{4}\left[\alpha_i|S_i| + \beta_i S_i^2\right]. \tag{39}$$

Since $\alpha_i > 0$ and $\beta_i > 0$ for $i = 1, 2, 3, 4$, we conclude that $\dot{V}$ is a strictly negative definite function defined on $\mathbb{R}^4$.

By Lyapunov stability theory, we have $S_i(t) \to 0$ for $i = 1, 2, 3, 4$ as $t \to \infty$.

Consequently, we see that $E_i(t) \to 0$ for $(i = 1, 2, 3, 4)$ as $t \to \infty$. ■

For MATLAB simulations, the parameters are taken as in the hyperchaotic case (5), *viz.* $a = 2.5$, $b = 2.5$, $c = 0.2$, $m = 1$ and $p = 0.2$.

The sliding constants for MATLAB simulations are regarded as $\alpha_i = 0.2$, $\beta_i = 8$ and $\nu_i = 10$ for $i = 1, 2, 3, 4$.

For the master system (M), we take the initial state as

$$y_1(0) = 3.9, \quad y_2(0) = 7.4, \quad y_3(0) = 10.3, \quad y_4(0) = 5.1. \tag{40}$$

For the slave system (S), we take the initial state as

$$z_1(0) = 15.4, \quad z_2(0) = 5.9, \quad z_3(0) = 6.2, \quad z_4(0) = 12.4. \tag{41}$$

The time-history for the synchronization errors between the master system (M) and the slave system (S) is depicted in Figure 15.

From Figure 15, we can see that the master system (M) and the slave system (S) are synchronised asymptotically for the initial states taken for the numerical simulation.

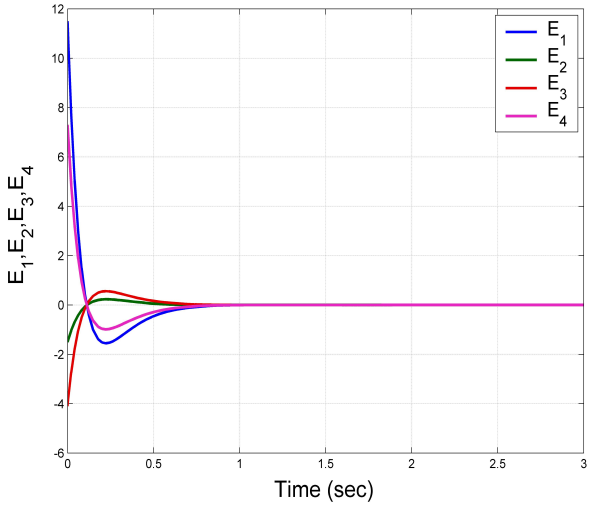

Figure 15: Asymptotic synchronisation of the master system (M) and the slave system (S) via integral sliding mode control (34)

7. Circuit simulation of the new 4D Hyperchaotic System

In this work, the new 4D hyperchaotic four-wing system (4) is realized by the NI MultiSIM 14.0 platform. The electronic circuit design of the hyperchaotic four-wing system is shown in Figure 16, in which AD633JN is selected as OPAMP. Applying the Kirchhoff's laws, the circuit presented in Figure 16 is described by the following equations:

$$\begin{cases} \dot{y_1} = \dfrac{1}{C_1R_1}y_1 + \dfrac{1}{C_1R_2}y_2 + \dfrac{1}{10C_1R_3}y_2y_3 - \dfrac{1}{C_1R_4}y_4\,, \\ \dot{y_2} = -\dfrac{1}{C_2R_5}y_1 + \dfrac{1}{10C_2R_6}y_2y_3 - \dfrac{1}{10C_2R_7}y_1y_3\,, \\ \dot{y_3} = -\dfrac{1}{C_3R_8}y_3 - \dfrac{1}{10C_3R_9}y_1y_2 - \dfrac{1}{10C_3R_{10}}y_2^2 + \dfrac{1}{C_3R_{11}}V_1\,, \\ \dot{y_4} = \dfrac{1}{C_4R_{12}}y_1\,. \end{cases} \tag{42}$$

Here y_1, y_2, y_3, y_4 are correspond to the voltages on the integrators U1A, U3A, U4A and U5A, respectively. The values of components in the circuit are selected as: $R_1 = 160$ kΩ, $R_2 = R_4 = R_8 = R_{12} = 400$ kΩ, $R_3 = R_6 = R_7 = R_9 = 40$ kΩ, $R_5 = 2$ MΩ, $R_{10} = 200$ kΩ, $R_{11} = 160$ kΩ, $R_{13} = R_{14} = R_{15} = R_{16} = R_{17} =$

$R_{18} = 100$ kΩ, $C_1 = C_2 = C_3 = C_4 = 3.2$ nF. MultiSIM outputs of the circuit are presented in Figure 17. These results are consistent with the Matlab simulation results shown in Figure 2.

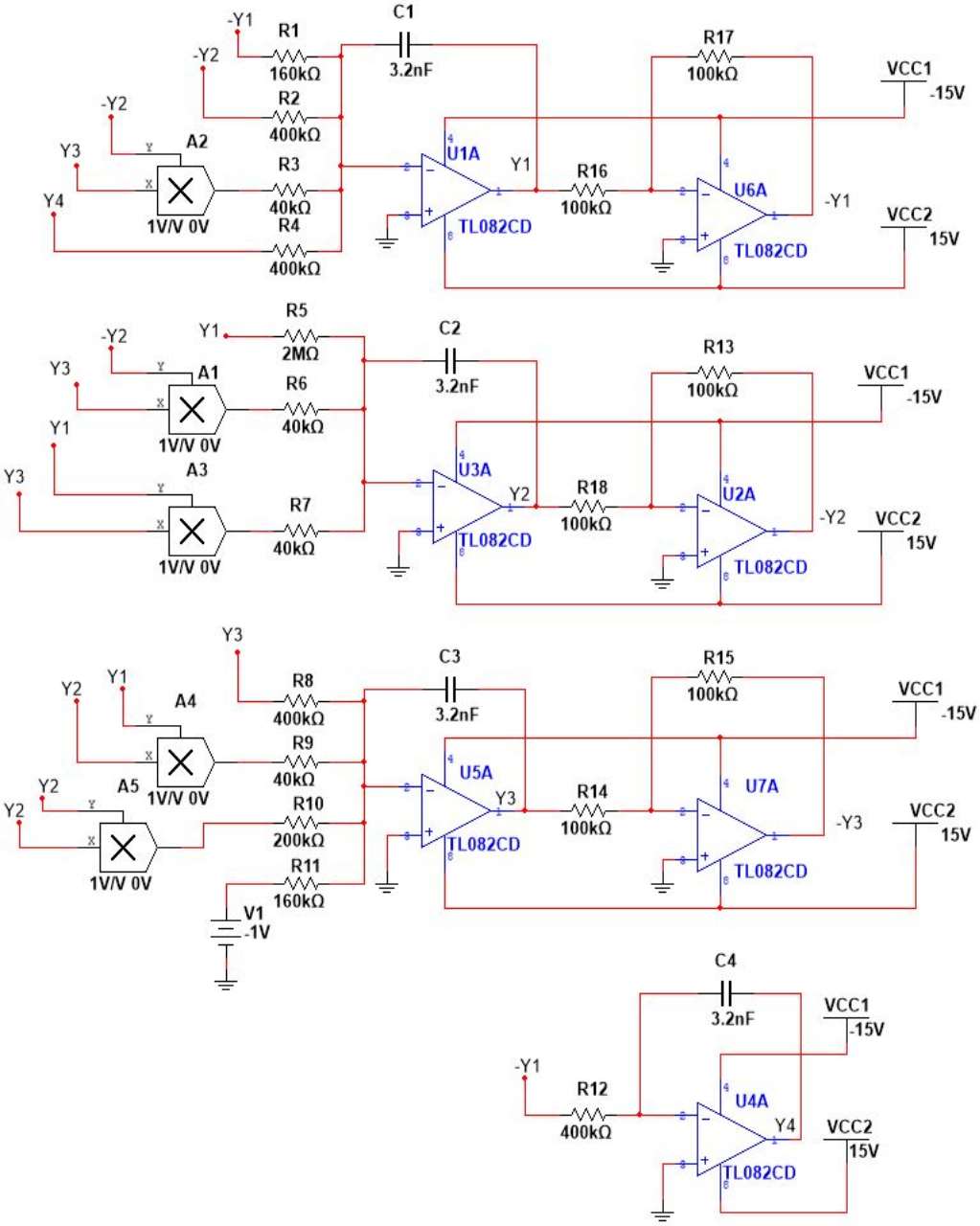

Figure 16: Circuit design of the new 4D hyperchaotic four-wing system (42)

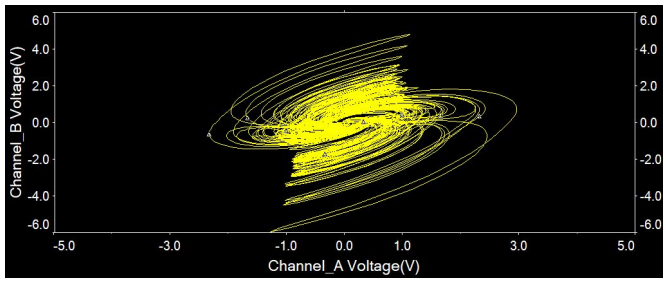

(a)

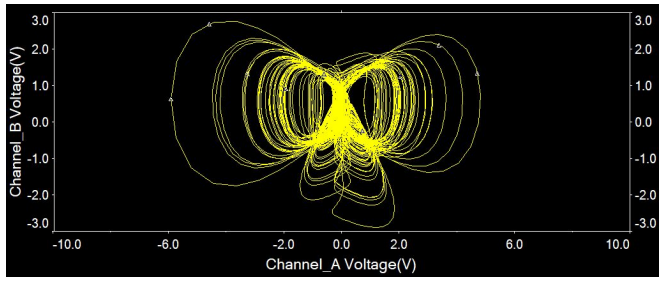

(b)

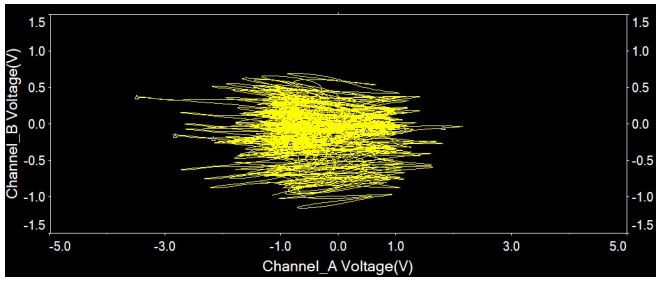

(c)

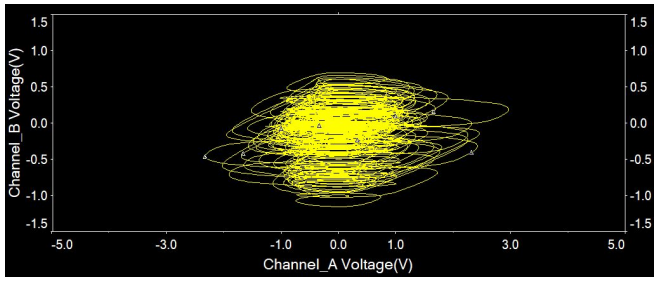

(d)

Figure 17: Hyperchaotic four-wing attractor of the new 4-D four-wing system (42 using MultiSim circuit simulation: (a) $y_1 - y_2$ plane, (b) $y_2 - y_3$ plane, (c) $y_3 - y_4$ plane and $y_1 - y_4$ plane

8. Conclusions

In this work, we modified the dynamics of 3-D four-wing Li chaotic system (Li *et al.* 2015) by introducing a feedback controller and derived a new 4-D hyperchaotic four-wing system with complex properties. We performed a detailed bifurcation analysis for the new hyperchaotic four-wing system and showed that the hyperchaotic four-wing system has multistability and coexisting attractors. We also investigated the offset-boosting properties of the new hyperchaotic four-wing system. Using integral sliding mode control, we got new results for the master-slave synchronization of hyperchaotic four-wing systems. Finally, we designed an electronic circuit using MultiSim which will be very useful for real implementation of the new hyperchaotic four-wing system.

References

[1] X. Peng, Y. Zeng, and Q. Xie: Dynamics analysis of a 5-dimensional hyperchaotic system with conservative flows under perturbation. *Chinese Physics B*, **30**(10) (2021), Article ID 100502. DOI: 10.1088/1674-1056/abea9a.

[2] F. Djimasra, J.D.D. Nkapkop, N. Tsafack, J. Kengne, J.Y. Effa, A. Boukabou, and L. Bitjoka: Robust cryptosystem using a new hyperchaotic oscillator with stricking dynamic properties. *Multimedia Tools and Applications*, **80**(16) (2021), 25121–25137. DOI: 10.1007/s11042-021-10734-1.

[3] J. Petrzela: Hyperchaotic self-oscillations of two-stage class C amplifier with generalized transistors. *IEEE Access*, **9** (2021), 62182–62194. DOI: 10.1109/ACCESS.2021.3074367.

[4] N.J. Mccullen and P. Moresco: Route to hyperchaos in a system of coupled oscillators with multistability. *Physical Review E*, **83**(4) (2011), Article ID 046212. DOI: 10.1103/PhysRevE.83.046212.

[5] H.A. Abdulkadhim and J.N. Shehab: Audio steganography based on least significant bits algorithm with 4D grid multi-wing hyper-chaotic system. *Interational Journal of Electrical and Computer Engineering*, **12**(1) (2022), 320–330. DOI: 10.11591/ijece.v12i1.pp320-330.

[6] M.D. Gupta and R.K. Chauhan: Secure image encryption scheme using 4D-Hyperchaotic systems based reconfigurable pseudo-random number generator and S-Box. *Integration*, **81** (2021), 137–159. DOI: 10.1016/j.vlsi.2021.07.002.

[7] Y.Y. Bian and W.X. Yu: A secure communication method based on 6-D hyperchaos and circuit implementation. *Telecommunication Systems*, **77**(4) (2021), 731–751. DOI: 10.1007/s11235-021-00790-1.

[8] M. Zhang, X. Tong, Z. Wang, and P. Chen: Joint lossless image compression and encryption scheme based on calic and hyperchaotic system. *Entropy*, **23** (8) (2021), Article ID 1096. DOI: 10.3390/e23081096.

[9] A. Khan and S. Kumar: Study of chaos in satellite system. *Pramana – Journal of Physics*, **90**(1) (2018), Article ID 0013. DOI: 10.1007/s12043-017-1502-0.

[10] C. Li, I. Pehlivan, J.C. Sprott, and A. Akgul: A novel four-wing strange attractor born in bistability. *IEICE Electronics Express*, **12**(4) (2015), Article ID 20141116. DOI: 10.1587/elex.12.20141116.

[11] Y. Deng and Y. Li: Bifurcation and bursting oscillations in 2D non-autonomous discrete memristor-based hyperchaotic map. *Chaos, Solitons and Fractals*, **150** (2021), Article ID 111064. DOI: 10.1016/j.chaos.2021.111064.

[12] C. Dong, K. Sun, S. He and H. Wang: A hyperchaotic cycloid map with attractor topology sensitive to system parameters. *Chaos*, **31** (8) (2021), Article ID 083132. DOI: 10.1063/5.0061519.

[13] H. Ming, H. Hu, and J. Zheng: Analysis of a new coupled hyperchaotic model and its topological types. *Nonlinear Dynamics*, **105** (2) (2021), 1937–1952. DOI: 10.1007/s11071-021-06692-w.

[14] S. Vaidyanathan, S. He, and A. Sambas: A new multistable double-scroll 4-D hyperchaotic system with no equilibrium point, its bifurcation analysis, synchronization and circuit design. *Archives of Control Sciences*, **31**(1) (2021), 99–128. DOI: 10.24425/acs.2021.136882.

[15] P.C. Rech: Hyperchaos and multistability in a four-dimensional financial mathematical model. *Journal of Applied Nonlinear Dynamics*, **10**(2) (2021), 211–218. DOI: 10.5890/JAND.2021.06.002.

[16] S. Vaidyanathan, I.M. Moroz, and A. Sambas: A new 4-D hyperchaotic system with no equilibrium, its multistability, offset boosting and circuit simulation. *Archives of Control Sciences*, **30**(3) (2020), 575–597. DOI: 10.24425/acs.2020.134678.

[17] L. Merah, A. Adnane, A. Ali-Pacha, S. Ramdani, and N. Hadj-Said: Real-time implementation of a chaos based cryptosystem on low-cost hardware. *Iranian Journal of Science and Technology – Transactions of Electrical Engineering*, **45**(4) (2021), 1127–1150. DOI: 10.1007/S40998-021-00433-W.

[18] M. Boumaraf and F. Merazka: Secure speech coding communication using hyperchaotic key generators for AMR-WB codec. *Multimedia Systems*, **27**(2) (2021), 247–269. DOI: 10.1007/s00530-020-00738-6.

[19] E. Zambrano-Serrano, J.M. Munoz-Pacheco, F.E. Serrano, L.A. Sanchez-Gaspariano, and C. Volos: Experimental verification of the multi-scroll chaotic attractors synchronization in PWL arbitrary-order systems using direct coupling and passivity-based control. *Integration*, **81** (2021), 56–70. DOI: 10.1016/j.vlsi.2021.05.012.

[20] S.L. Yan: Synchronizations of quasi-period and hyperchaos in injected two-section semiconductor lasers. *Journal of Optical Communications*, **34**(1) (2013), 9–14. DOI: 10.1515/joc-2013-0003.

[21] R.J. Yahya and N.H. Abbas: Optimal integral sliding mode controller controller design for 2-RLFJ manipulator based on hybrid optimization algorithm. *International Journal of Electrical and Computer Engineering*, **12**(1) (2022), 293–302. DOI: 10.11591/ijece.v12i1.pp293-302.

[22] G.P. Incremona, L. Mirkin, and P. Colaneri: Integral sliding-mode control with internal model: A separation. *IEEE Control Systems Letters*, **6** (2022), 446–451. DOI: 10.1109/LCSYS.2021.3079187.

[23] G. Xu, S. Zhao, and Y. Cheng: Chaotic synchronization based on improved global nonlinear integral sliding mode control. *Computers and Electrical Engineering*, **96** (2021), Article ID 107497. DOI: 10.1016/j.compeleceng.2021.107497.

[24] S. Kumar, C. Singh, S.N. Prasad, C. Shekhar, and R. Aggarwal: Synchronization of fractional order Rabinovich-Fabrikant systems using sliding mode control techniques. *Archives of Control Sciences*, **29**(2), (2019), 307–322. DOI: 10.24425/acs.2019.129384.

[25] A. Ouannas, A.T. Azar, and S. Vaidyanathan: A robust method for new fractional hybrid chaos synchronization. *Mathematical Methods in the Applied Sciences*, **40**(5), (2017), 1804–1812. DOI: 10.1002/mma.4099.

[26] S. Vaidyanathan: A ten-term novel 4-D hyperchaotic system with three quadratic nonlinearities and its control. *International Journal of Control Theory and Applications*, **6**(2), (2013), 97–109.

[27] A. Sambas, S. Vaidyanathan, X. Zhang, I. Koyuncu, T. Bonny, M. Tuna, M. Alcin, S. Zhang, I.M. Sulaiman, A.M. Awwal, and P. Kumam: A novel 3D chaotic system with line equilibrium: Multistability, integral sliding mode control, electronic circuit, FPGA implementation and its image encryption. *IEEE Access*, **10** (2022), 68057–68074. DOI: 10.1109/ACCESS.2022.3181424.

[28] S. Vaidyanathan, K. Benkouider, and A. Sambas: A new multistable jerk chaotic system, its bifurcation analysis, backstepping control-based synchronization design and circuit simulation. *Archives of Control Sciences*, **32**(1), (2022), 123–152. DOI: 10.24425/acs.2022.140868.

[29] X. Zhou, C. Li, X. Lu, T. Lei, and Y. Zhao: A 2D hyperchaotic map: Amplitude control, coexisting symmetrical attractors and circuit implementation. *Symmetry*, **13** (6) (2021), Article ID 1047. DOI: 10.3390/sym13061047.

[30] J. Luo, S. Qu, Y. Chen, X. Chen, and Z. Xiong: Synchronization, circuit and secure communication implementation of a memristor-based hyperchaotic system using single input controller. *Chinese Journal of Physics*, **71** (2021), 403–417. DOI: 10.1016/j.cjph.2021.03.009.